THE ASTROPHYSICAL JOURNAL SUPPLEMENT SERIES, 128:549–560, 2000 June
© 2000. American Astronomical Society. All rights reserved. Printed in U.S.A.

THE *ULYSSES* SUPPLEMENT TO THE *GRANAT*/WATCH CATALOG OF COSMIC GAMMA-RAY BURSTS

K. HURLEY
University of California, Berkeley, Space Sciences Laboratory, Berkeley, CA 94720-7450
N. LUND AND S. BRANDT
Danish Space Research Institute, DK-2100 Copenhagen, Denmark
C. BARAT
Centre d'Étude Spatiale des Rayonnements, F-31029 Toulouse Cedex, France
T. CLINE
NASA Goddard Space Flight Center, Greenbelt, MD 20771
R. SUNYAEV, O. TEREKHOV, A. KUZNETSOV, AND S. SAZONOV
Institut Kosmitcheskij Isledovanja, 117810 Moscow, Russia
AND
A. CASTRO-TIRADO[1]
Laboratorio de Astrofísica Espacial y Física Fundamental (LAEFF-INTA), P.O. Box 50727, E-28080 Madrid, Spain
Received 2000 January 3; accepted 2000 February 9

ABSTRACT

We present third Interplanetary Network (IPN) localization data for 56 gamma-ray bursts in the *Granat*/WATCH catalog that occurred between 1990 November and 1994 September. These localizations are obtained by triangulation using various combinations of spacecraft and instruments in the IPN, which consisted of *Ulysses*, BATSE, *Pioneer Venus Orbiter*, *Mars Observer*, WATCH, and PHEBUS. The intersections of the triangulation annuli with the WATCH error circles produce error boxes with areas as small as 16 arcmin^2, reducing the sizes of the error circles by factors of up to 800.

Subject headings: catalogs — gamma rays: bursts

1. INTRODUCTION

The multiwavelength counterparts to numerous gamma-ray bursts (GRBs) have now been identified using the rapid, precise localizations available from the *BeppoSAX* spacecraft (e.g., Costa et al. 1997; van Paradijs et al. 1997), as well as from the *Rossi X-Ray Timing Explorer* and the Interplanetary Network. However, there is still a need for less precise GRB localizations of older bursts, for several reasons. For example, the discovery of bright optical emission coincident with one burst (Akerlof et al. 1999) indicates that searches through archival optical data may reveal other examples of this interesting phenomenon. Also, the possible association of one GRB with a nearby supernova (Galama et al. 1998), if valid, means that other such associations may exist in the historical records. Because the current rate of rapid, precise localizations remains low ($\sim$eight events yr^{-1}), it is important to add as many bursts as possible to the existing database. The *Granat*/WATCH GRB catalog contains data on 95 bursts observed between 1989 and 1994 (Sazonov et al. 1998); of the 95, 47 bursts were localized to error circles with radii between 0.°2 and 1.°6. The third Interplanetary Network (IPN) began operations in 1990 with the launch of the *Ulysses* spacecraft. By combining WATCH data with IPN data, it is possible to reduce the sizes of these error circles by as much as a factor of 800, making them more useful for archival studies. This is the seventh in a series of catalogs of IPN localizations. The supplements to the BATSE 3B and 4Br catalogs appeared in Hurley et al. (1999a, 1999b; 218 and 147 bursts, respectively). Localizations involving the *Mars Observer* (*MO*) and *Pioneer Venus Orbiter* (*PVO*) spacecraft have been presented in Laros et al. (1997, 1998; nine and 37 bursts, respectively). Fifteen *Ulysses*, *PVO*, SIGMA, WATCH, and PHEBUS burst localizations were published in Hurley et al. (2000a). *Ulysses*/*BeppoSAX* bursts may be found in Hurley et al. (2000b; 16 bursts). Localization data for the bursts in all these catalogs may also be found on the IPN Web site.[2]

2. INSTRUMENTATION

The gamma-ray bursts in this paper were observed by at least two instruments. One was the omnidirectional GRB detector aboard the *Ulysses* spacecraft, consisting of two 3 mm thick hemispherical CsI scintillators with a projected area of $\sim$20 cm^2 in any direction. The instrument observes bursts in the 25–150 keV energy range in either a triggered mode, in which the time resolution is as high as 8 ms, or, for the weaker bursts, in a real-time mode, in which the time resolution is between 0.25 and 2 s. A more complete description of the experiment may be found in Hurley et al. (1992).

The second was the WATCH experiment aboard the *Granat* spacecraft. WATCH employs a unique rotating modulation collimator technique to determine the positions of bursts to $\sim 1^\circ$ accuracy. The detector is a scintillator operating in the 8–60 keV range with a field of view of 74° and a maximum effective area of 47 cm^2. Four independent modules were deployed aboard the *Granat* spacecraft, and $\sim$80% of the sky was monitored with them. See Sazonov et al. (1998) for a more detailed description.

[1] Instituto de Astrofísica de Andalucía (IAA-CSIC), P.O. Box 03004, E-18080 Granada, Spain.

[2] ssl.berkeley.edu/ipn3/index.html.

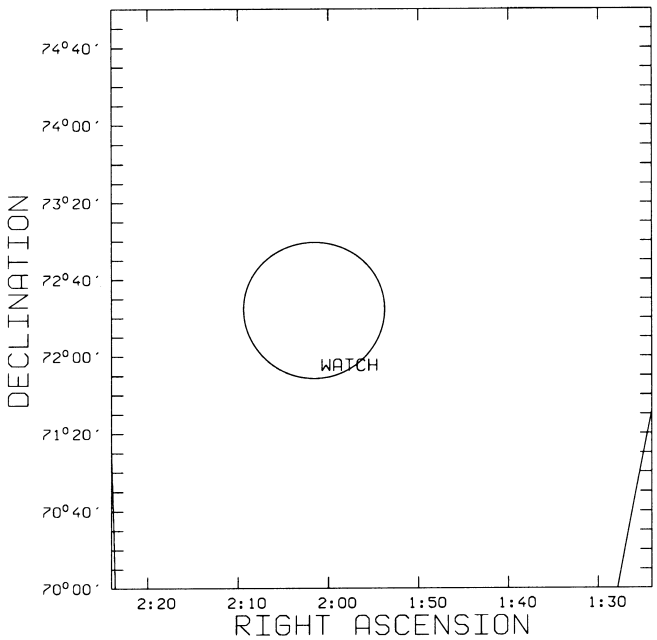

FIG. 1.—IPN 3 σ annulus and WATCH 3 σ error circle for 901121. The large width of the annulus, just visible in the lower part of the figure, is due to the fact that *Ulysses* had just been launched and was only 67 lt-s from Earth.

To localize the GRBs in this supplement, use was sometimes made of the data from other experiments, too. These are noted in the following section.

3. TECHNIQUE

The methodology employed here is similar or identical to that used for the *Ulysses* supplement to the BATSE 3B and 4Br catalogs (Hurley et al. 1999a, 1999b). Each WATCH burst was searched for in the *Ulysses* data. One or more annuli of possible arrival directions was derived by triangulation for each burst identified using the data from *Ulysses* and at least one other instrument. The bursts in this catalog thus fall into one of the following categories:

1. Event observed by *Ulysses* and WATCH only. In this case, the triangulation annulus was obtained utilizing the data of these two instruments.

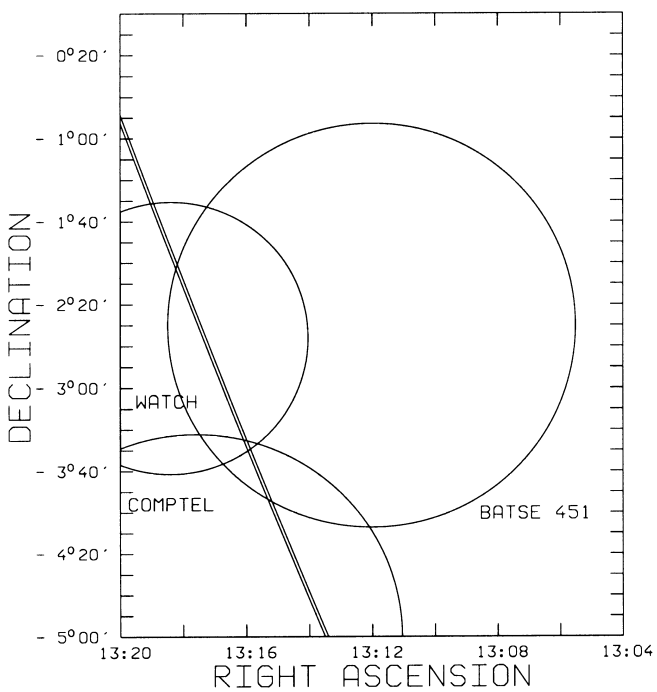

FIG. 2.—IPN annulus (3 σ), COMPTEL (1 σ), WATCH (3 σ), and BATSE (1 σ) error circles for 910627.

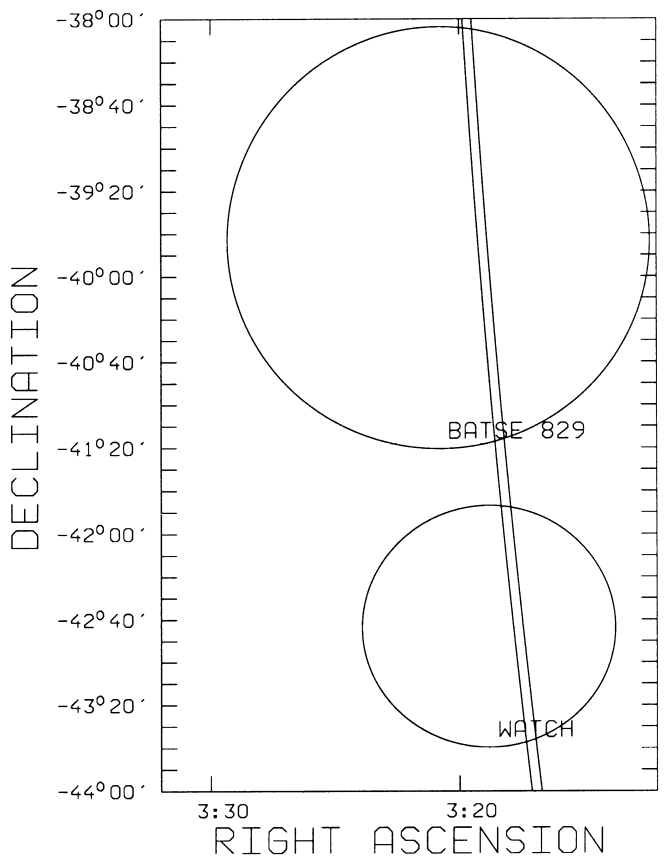

FIG. 3.—IPN annulus (3 σ), WATCH (3 σ), and BATSE (1 σ) error circles for 910927.

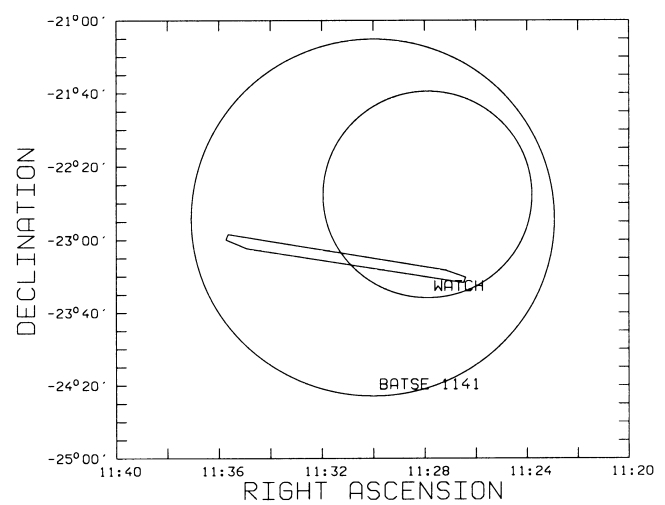

FIG. 4.—*PVO*/*Ulysses*/BATSE 3 σ error box from Laros et al. (1998), WATCH 3 σ error circle, and BATSE 1 σ error circle for 911202.

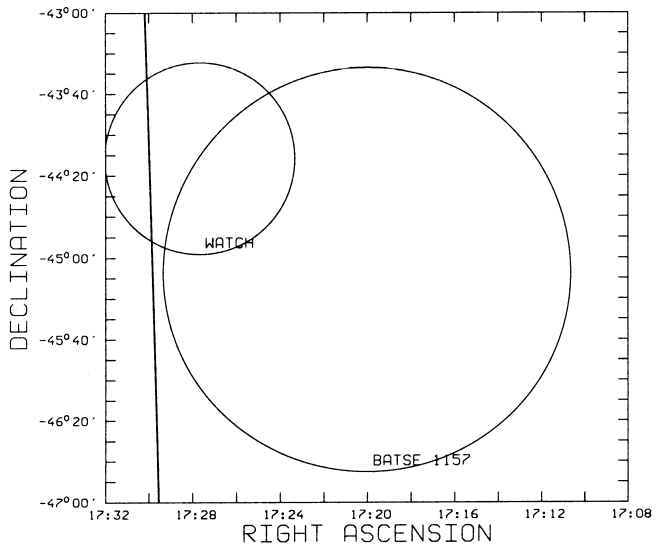

FIG. 5.—IPN annulus (3 σ), WATCH (3 σ), and BATSE (1 σ) error circles for 911209.

2. Event observed by *Ulysses*, WATCH, and PHEBUS. PHEBUS was also aboard the *Granat* spacecraft (Barat et al. 1988; Terekhov et al. 1991). It consisted of six 12 cm long by 7.8 cm diameter BGO detectors oriented along the axes of a Cartesian coordinate system, operating in the 100 keV–100 MeV energy range, with 1/128 s to 1/32 s time resolution. In this case, the triangulation was done using *Ulysses* and the instrument that resulted in the most precise triangulation annulus. The WATCH data have the advantage of being taken in an energy range that corresponds more closely to that of *Ulysses*, but the time resolution of the WATCH data was sometimes rather coarse ($\sim$10 s or more). On the other hand, the PHEBUS data, although taken in an energy range higher than that of *Ulysses*, have the advantages of good time resolution and in some cases better statistics. The more accurate of the two possible triangulation annuli is quoted here.

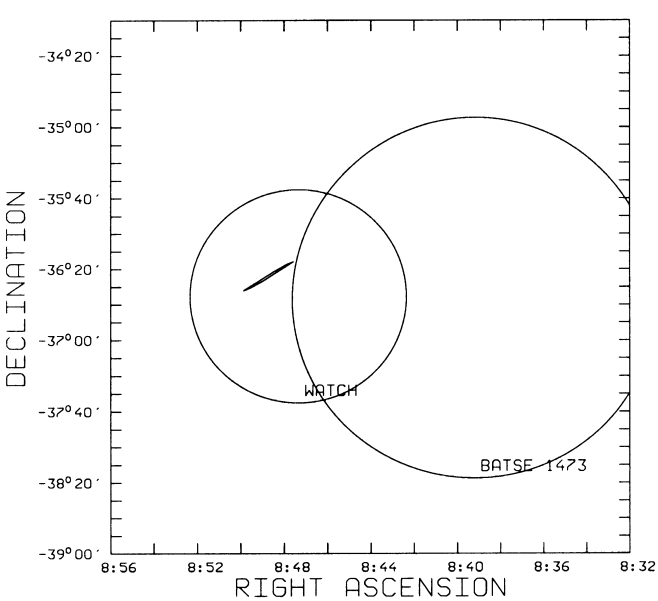

FIG. 6.—*PVO*/*Ulysses*/BATSE error box (3 σ) from Laros et al. (1998), WATCH error circle (3 σ), and BATSE error circle (1 σ) for 920311.

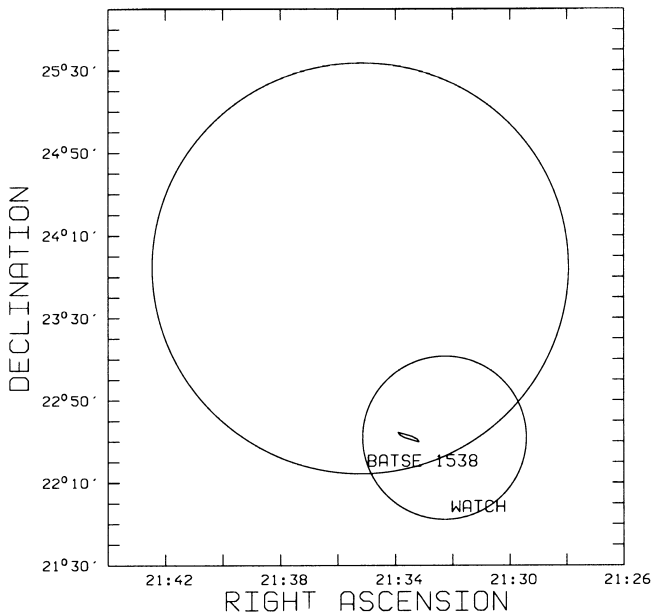

FIG. 7.—*PVO*/*Ulysses*/BATSE error box (3 σ) from Laros et al. (1998), WATCH error circle (3 σ), and BATSE error circle (1 σ) for 920404.

3. Event observed by *Ulysses*, WATCH, and BATSE. BATSE consists of eight detector modules aboard the *Compton Gamma-Ray Observatory* (*CGRO*). Each module has an area $\sim$2025 cm^2. The DISCSC data type was used, which gives 0.064 ms resolution data for the 25–100 keV energy range. BATSE is described in Meegan et al. (1996). For the purposes of triangulation, the *Granat* and *CGRO* spacecraft were close enough to one another ($<$250 lt-ms) that the accuracy of the triangulation could not be improved by including the data from both spacecraft. (For comparison, the *Ulysses*-Earth distance was as great as several thousand light-seconds.) In this case, the *Ulysses*-BATSE annulus was used since the BATSE energy range corresponds closely to that of *Ulysses*, the time resolution is good, and the statistics are always better. These annuli have appeared in Hurley et al. (1999a), but their intersections with the WATCH error circles are presented here for the first time. The BATSE error circles may be found in Meegan et al. (1996) and in the revised 4Br catalog of Paciesas et al.

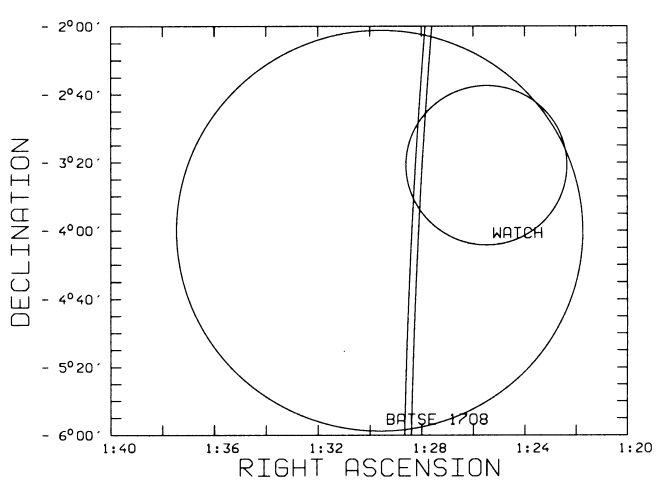

FIG. 8.—IPN annulus (3 σ), WATCH (3 σ), and BATSE (1 σ) error circles for the burst of 920718 at 14:40.

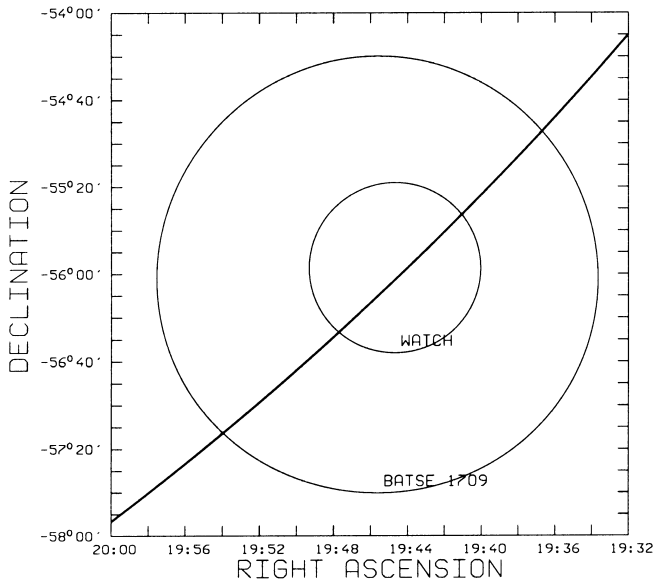

FIG. 9.—IPN annulus (3 σ), WATCH (3 σ), and BATSE (1 σ) error circles for the burst of 920718 at 21:32.

(1999). The radii of the error circles presented here include both statistical and systematic errors. In those cases where WATCH did not localize the burst, the *Ulysses*-BATSE localization information consists of the intersection of the IPN annulus with BATSE error circle. Because the error circle is large, the curvature of the annulus does not allow a simple description of the error box, and no localization information appears in Table 2; it may be found in Hurley et al. (1999a).

4. Event observed by *Ulysses*, WATCH, and one or more of the following experiments: BATSE, COMPTEL (Kippen et al. 1998), SIGMA (Claret et al. 1994), *PVO* (Laros et al. 1997), or *MO* (Laros et al. 1998). Here triangulation using *PVO* or *MO* data, and/or the independent localization capabilities of COMPTEL or SIGMA, have been utilized. These special cases are noted in Table 2, and the previously published error box coordinates have been included in the table for convenience. In most cases the error box is fully contained within the WATCH error circle. If no figure has been previously published showing the WATCH error circle and the IPN triangulation result, one appears in this paper.

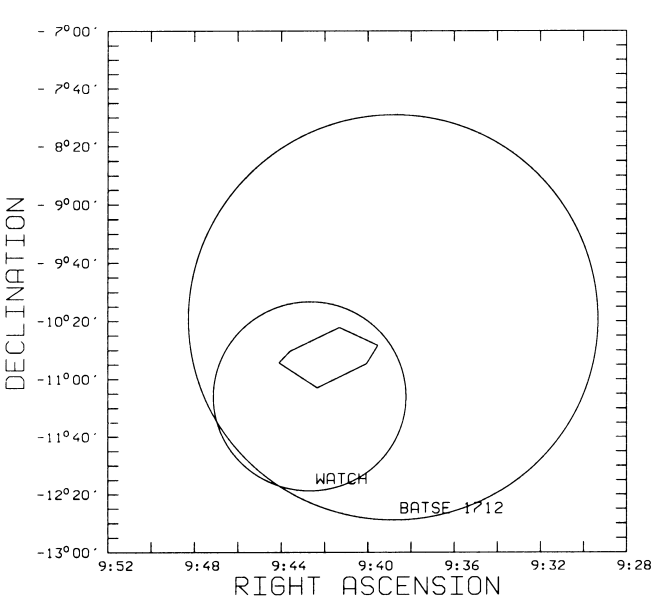

FIG. 10.—*PVO*/*Ulysses*/BATSE error box (3 σ) from Laros et al. (1998), WATCH error circle (3 σ), and BATSE error circle (1 σ) for 920720.

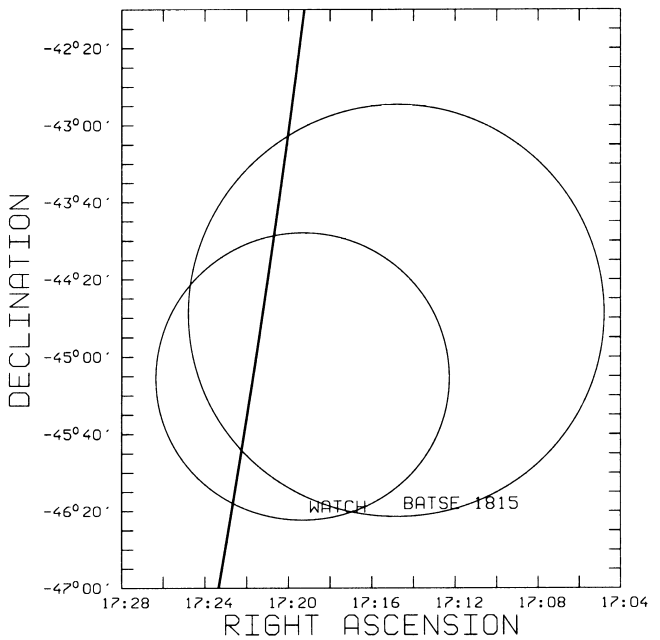

FIG. 11.—IPN annulus (3 σ), WATCH (3 σ), and BATSE (1 σ) error circles for 920814.

4. THE DATA

In Table 1 the WATCH bursts also detected by *Ulysses* are listed. Column (1) gives the date, column (2) gives the detection time at WATCH, and column (3) indicates the *Ulysses* data mode (RI for rate increase, observed in the low

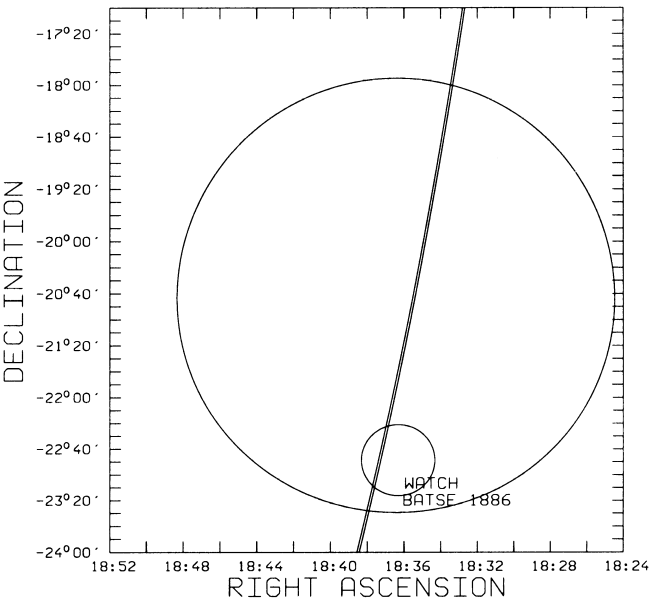

FIG. 12.—IPN annulus (3 σ), WATCH (3 σ), and BATSE (1 σ) error circles for 920902.

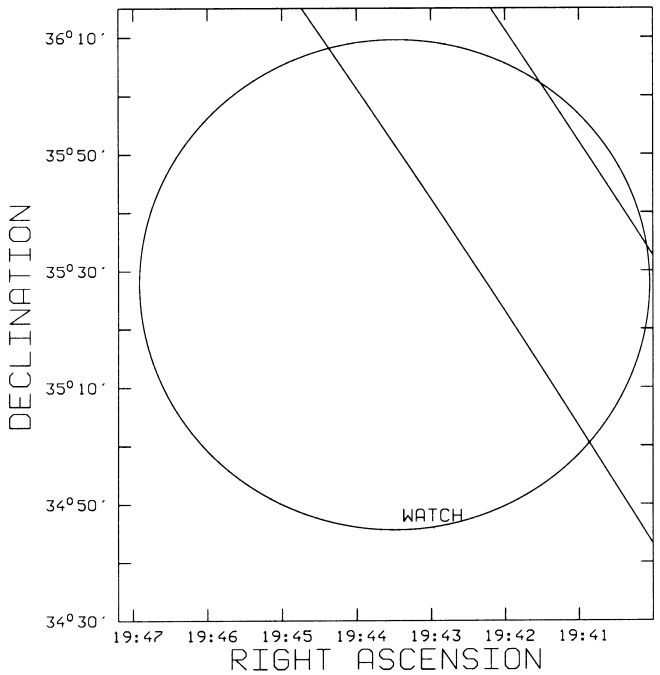

FIG. 13.—IPN annulus (3 σ) and WATCH error circle (3 σ) for the burst of 920903 at 01:37.

time resolution real-time mode, trigger for the high time resolution triggered mode). Column (4) indicates whether BATSE observed the burst. Here N/O means not observable (*CGRO* had not been launched yet), and a number, if present, is the BATSE trigger number. Column (5) indicates whether the burst was localized by WATCH, and column (6) indicates whether PHEBUS observed the event.

Table 2 gives the localization information for the events in Table 1. Columns (1) and (2) give the date and the time. For those bursts localized by WATCH, columns (3) and (4) give the right ascension and declination of the center of the WATCH error circle (J2000), and column (5) gives the

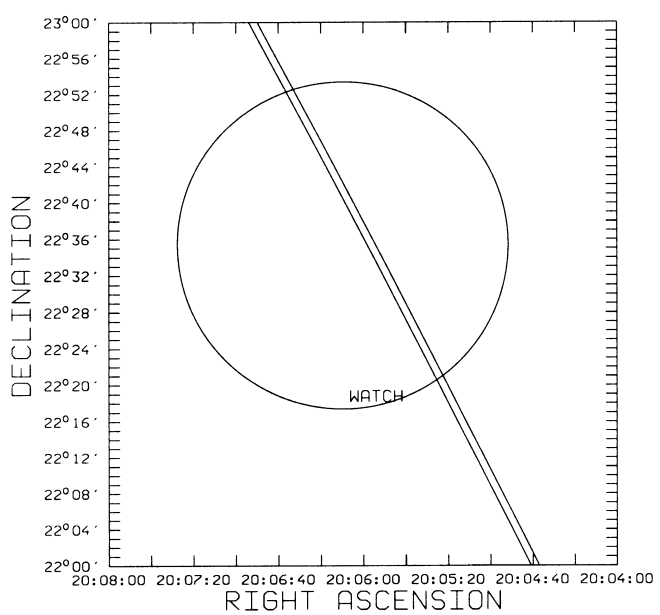

FIG. 14.—IPN annulus (3 σ) and WATCH error circle (3 σ) for the burst of 920903 at 23:29.

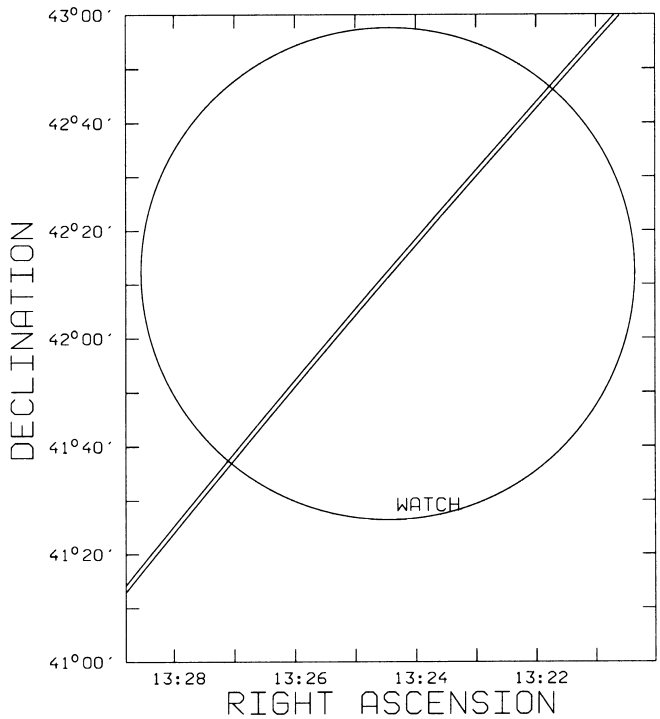

FIG. 15.—IPN annulus (3 σ) and WATCH error circle (3 σ) for the burst of 920925 at 20:30.

WATCH 3 σ error circle radius. These data are taken directly from Sazonov et al. (1998), and the error circle radius includes both statistical and systematic errors. Columns (6) and (7) give the right ascension and declination (α, δ) of the center of the IPN annulus (J2000); columns (8) and (9) give the radius R of the center line of the annulus and the 3 σ half-width of the annulus δR. That is, the annulus is described by two small circles on the celestial sphere both centered at α, δ, with radii $R - \delta R$ and $R + \delta R$. The annulus half-width is calculated taking both statistical and systematic errors into account. For those cases where there is a WATCH error circle and the annulus intersects it, additional data are given in columns (10) and (11). (The possible exceptions are, first, cases where the IPN annulus is wider than the error circle diameter and therefore does not intersect it and, second, cases where an actual error box has

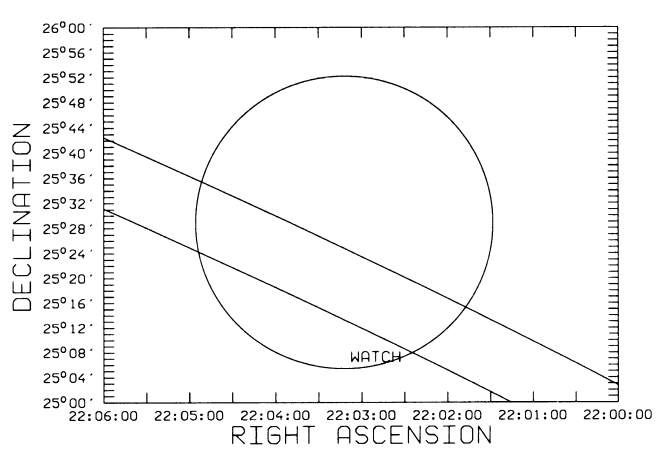

FIG. 16.—IPN annulus (3 σ) and WATCH error circle (3 σ) for the burst of 920925 at 22:46.

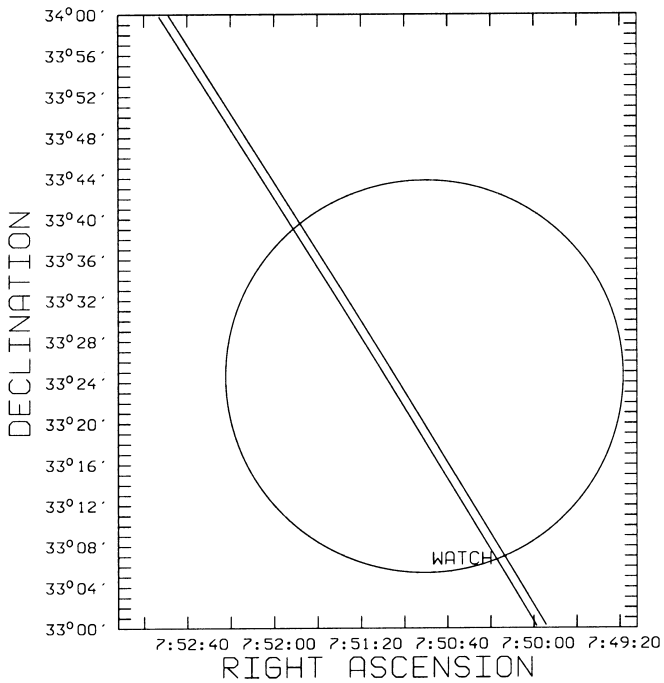

FIG. 17.—IPN annulus (3 σ) and WATCH error circle (3 σ) for 921013.

been obtained and published elsewhere.) Column (10) gives the right ascensions and declinations (J2000) of the IPN error box, and column (11) gives the error box area. Note that, strictly speaking, it is not possible to define a true error

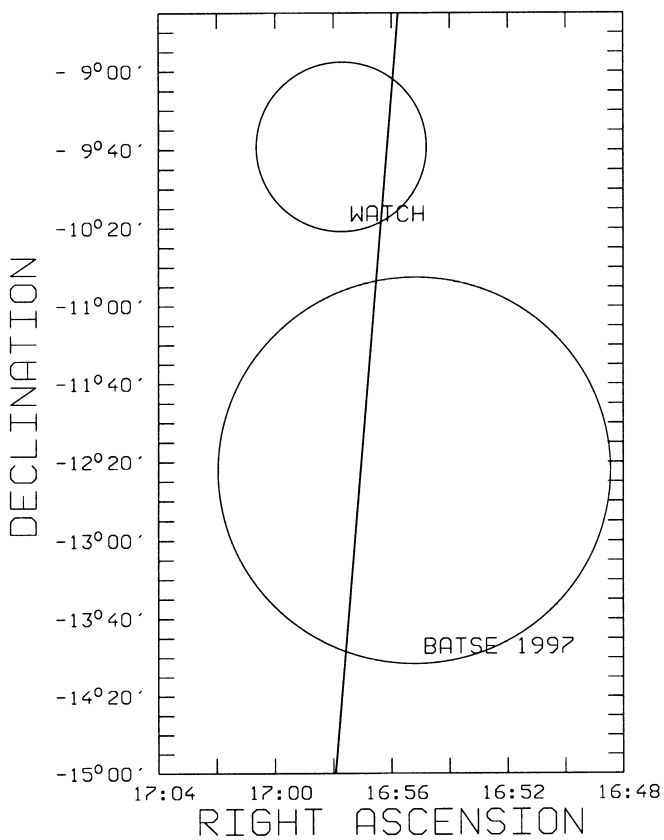

FIG. 18.—IPN annulus (3 σ), BATSE (1 σ), and WATCH (3 σ) error circles for 921022.

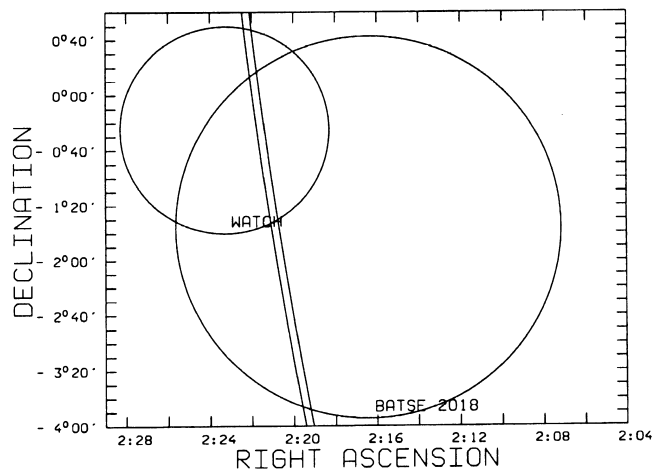

FIG. 19.—IPN annulus (3 σ), BATSE (1 σ), and WATCH (3 σ) error circles for 921029.

box with straight line segments among the four intersection points of a WATCH error circle with an IPN annulus due to the curvatures of both the annulus and the error circle. However, for many purposes, this may be negligible.

5. DISCUSSION AND CONCLUSIONS

There is good agreement between the IPN annuli and the WATCH error circles in all cases. We call attention to some of the more precise error boxes:

1. *940703.*—The error box area is 16 arcmin^2, a reduction in area from the 0.°24 WATCH error circle of a factor of $\sim$41.

2. *921022.*—The error box area is 22 arcmin^2, a reduction in area from the 0.°72 WATCH error circle of a factor of $\sim$265.

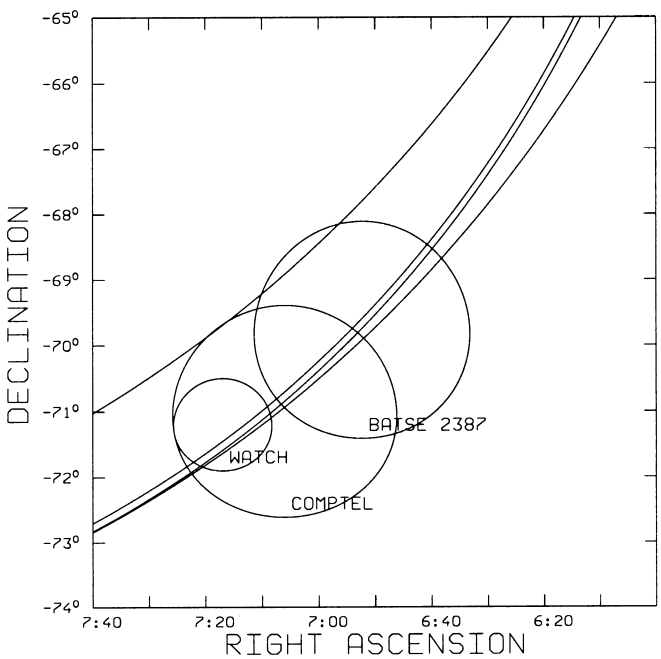

FIG. 20.—IPN 3 σ annuli (*Ulysses*/BATSE/*MO*) and BATSE (1 σ), COMPTEL (1 σ), and WATCH (3 σ) error circles for 930612. The narrow inner IPN annulus and the wider outer IPN annulus intersect outside the figure to form a long error box.

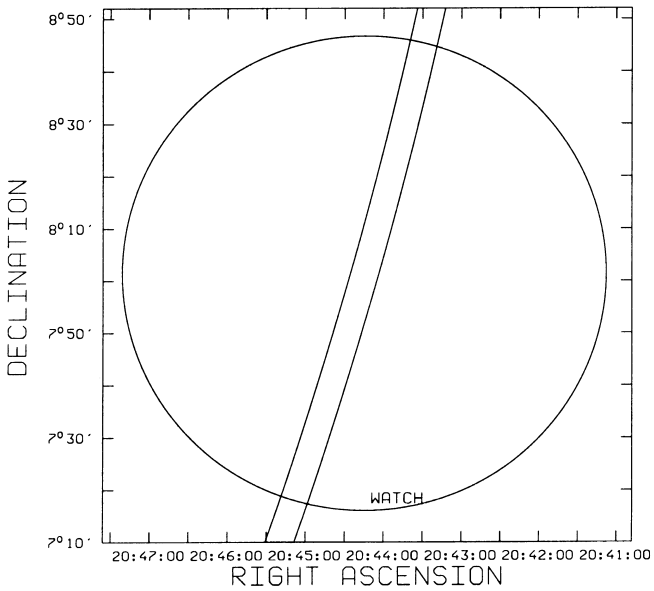

FIG. 21.—IPN annulus (3 σ) and WATCH error circle (3 σ) for 930703.

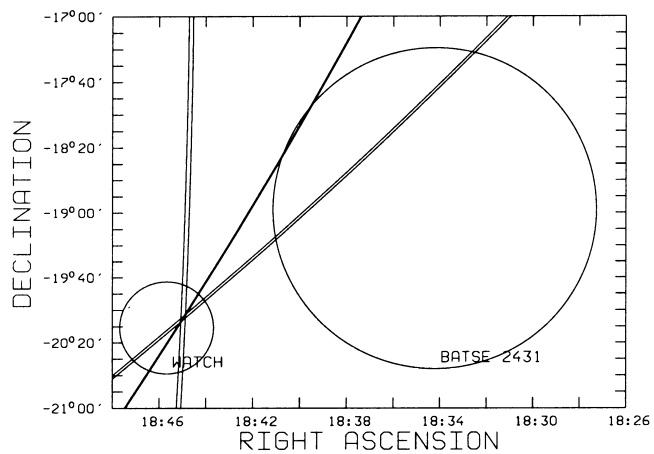

FIG. 22.—IPN 3 σ annuli (*Ulysses*/BATSE/*MO*), BATSE (1 σ), and WATCH (3 σ) error circles for 930706.

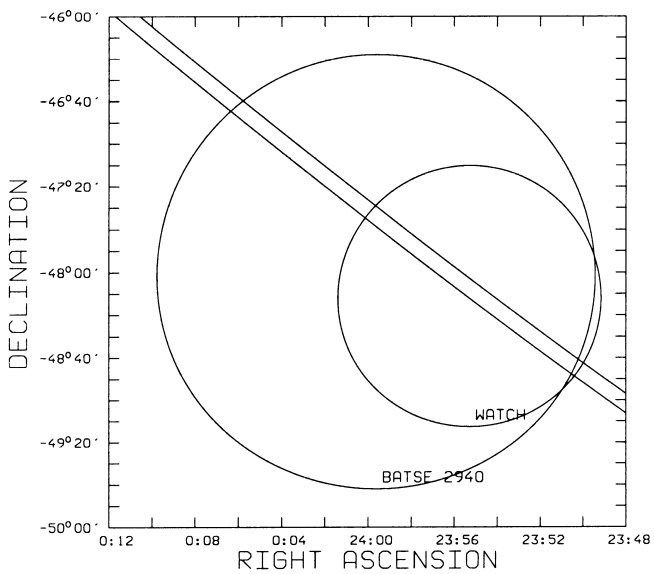

FIG. 23.—IPN annulus (3 σ), WATCH (3 σ), and BATSE (1 σ) error circles for 940419.

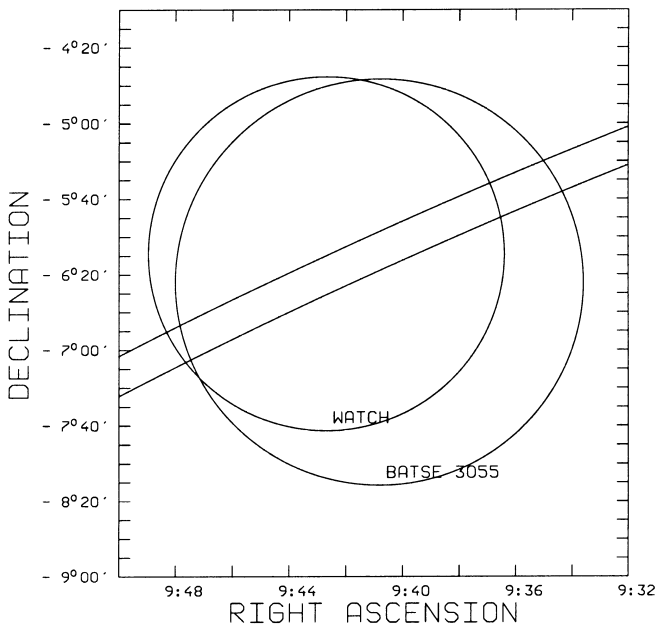

FIG. 24.—IPN annulus (3 σ), WATCH (3 σ), and BATSE (1 σ) error circles for the burst of 940701.

3. *921013*.—The error box area is 32 arcmin^2, a reduction in area from the 1°.51 WATCH error circle of a factor of $\sim$800.

The localizations in Table 2 are presented in Figures 1–25. (Figures for the WATCH bursts involving SIGMA, which have already appeared in Hurley et al. 2000a, have been omitted.) As these figures show, the combination of WATCH and the IPN results in very precise location information for these bursts. Another version of the WATCH experiment was flown aboard the *EURECA* spacecraft. Analysis of these events is currently underway.

K. H. is grateful to J. P. L. for *Ulysses* support under contract 958056 and to NASA for Compton Gamma-Ray Observatory support under grant NAG 5-3811.

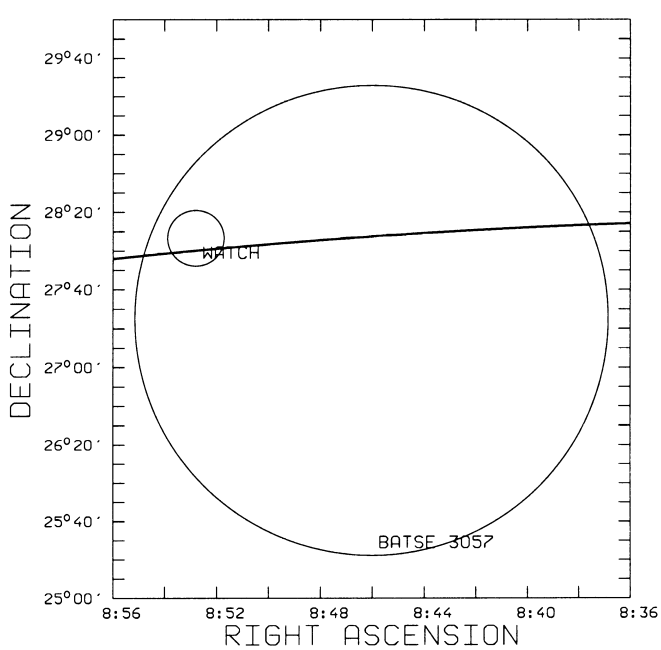

FIG. 25.—IPN annulus (3 σ), WATCH (3 σ), and BATSE (1 σ) error circles for the burst of 940703.

TABLE 1

ULYSSES-WATCH BURSTS

Date (1)	Time (UT) (2)	*Ulysses* (3)	BATSE (4)	WATCH (5)	PHEBUS (6)
1990 Nov 12	14:57:41	RI	N/O	No	Yes
1990 Nov 21	18:07:11	RI	N/O	Yes	Yes
1991 Jan 17	0:58:13	RI	N/O	No	Yes
1991 Jan 22	15:14:00	Trigger	N/O	Yes	Yes
1991 Feb 19	11:45:24	Trigger	N/O	Yes	N/O
1991 Mar 10	13:02:03	Trigger	N/O	Yes	N/O
1991 Apr 25	0:38:05	RI	109	No	No
1991 May 17.....	5:02:38	RI		No	Yes
1991 Jun 27.....	4:29:23	Trigger	451	Yes	Yes
1991 Jul 17.....	4:33:06	Trigger	543	No	Yes
1991 Jul 17.....	13:07:23	Trigger		No	N/O
1991 Jul 21.....	19:30:17	RI	563	No	No
1991 Aug 14	19:14:38	RI	678	No	Yes
1991 Aug 15	12:34:25	RI		No	No
1991 Sep 27.....	23:27:00	Trigger	829	Yes	N/O
1991 Oct 16.....	11:01:34	RI	907	Yes	Yes
1991 Oct 22.....	4:14:00	RI	914	No	No
1991 Dec 2.....	20:28:51	Trigger	1141	Yes	N/O
1991 Dec 9.....	18:36:11	Trigger	1157	Yes	N/O
1992 Mar 7	0:18:11	RI	1467	No	No
1992 Mar 11	2:20:26	Trigger	1473	Yes	Yes
1992 Mar 25	17:17:37	Trigger	1519	No	Yes
1992 Apr 4.....	13:11:45	Trigger	1538	Yes	N/O
1992 Jul 11.....	16:09:17	Trigger	1695	No	N/O
1992 Jul 14.....	13:04:33	RI	1698	Yes	Yes
1992 Jul 18.....	14:40:43	RI	1708	Yes	No
1992 Jul 18.....	21:32:44	Trigger	1709	Yes	Yes
1992 Jul 20.....	5:53:20	RI	1712	Yes	No
1992 Jul 23.....	1:00:49	Trigger	1721	No	Yes
1992 Jul 23.....	20:03:09	Trigger		Yes	Yes
1992 Aug 14	6:10:35	RI	1815	Yes	No
1992 Sep 2	0:29:02	Trigger	1886	Yes	Yes
1992 Sep 3	1:35:46	RI		Yes	Yes
1992 Sep 3	23:29:01	Trigger		Yes	Yes
1992 Sep 25.....	20:30:42	RI		Yes	Yes
1992 Sep 25.....	21:45:20	RI	1956	No	No
1992 Sep 25.....	22:46:24	RI		Yes	No
1992 Oct 13.....	23:00:42	Trigger		Yes	Yes
1992 Oct 22.....	15:21:00	Trigger	1997	Yes	N/O
1992 Oct 25.....	13:55:40	Trigger		No	Yes
1992 Oct 29.....	12:38:05	RI	2018	Yes	No
1993 Jan 6	15:37:40	Trigger	2121	No	Yes
1993 Jan 16	2:47:06	RI	2136	No	No
1993 Jun 9	10:07:30	RI	2383	No	No
1993 Jun 12.....	0:44:20	RI	2387	Yes	Yes
1993 Jul 3	11:26:30	Trigger		Yes	N/O
1993 Jul 5	12:39:18	RI	2429	No	No
1993 Jul 6	5:13:31	Trigger	2431	Yes	Yes
1993 Jul 14.....	16:13:04	RI	2446	No	Yes
1993 Sep 10.....	12:12:30	RI	2522	No	No
1993 Sep 27.....	4:18:15	RI	2542	No	No
1994 Mar 29	18:15:44	RI	2897	No	No
1994 Apr 19	19:11:07	RI	2940	Yes	Yes
1994 Jun 19.....	21:32:32	RI	3035	No	Yes
1994 Jul 1	21:44:29	RI	3055	Yes	No
1994 Jul 3	4:40:55	Trigger	3057	Yes	Yes
1994 Sep 10.....	23:57:56	Trigger		No	Yes

TABLE 2

LOCALIZATIONS

DATE (1)	TIME (UT) (2)	WATCH α (3)	WATCH δ (4)	WATCH R (5)	IPN α (6)	IPN δ (7)	IPN R (8)	IPN δR (9)	ERROR BOX CORNERS (α, δ) (10)	AREA (arcmin²) (11)
1990 Nov 12	14:57:41				115.525	28.474	48.575	0.678		
1990 Nov 21	18:07:11	30.39	72.40	0.59	113.042	28.773	61.102	2.369		
1991 Jan 17	0:58:13				95.972	27.621	64.757	0.629		
1991 Jan 22[a]	15:14:00	297.48	−71.23	0.69					296.918, −70.681	
									296.595, −70.612	
									296.674, −70.660	
									296.838, −70.633	
									297.000, −70.667	
									296.512, −70.626	18
1991 Feb 19[a]	11:45:24	212.94	58.54	0.95					213.731, 58.671	
									213.657, 58.705	
									213.723, 58.710	
									213.665, 58.666	
									213.701, 58.649	
									213.687, 58.727	7.3
1991 Mar 10[a]	13:02:03	184.10	6.38	0.55					184.358, 7.266	
									184.249, 7.125	
									184.198, 6.921	
									184.405, 7.462	
									184.424, 7.480	
									184.178, 6.901	63
1991 Apr 25[b]	00:38:05									
1991 May 17[a]	05:02:38								150.475, −42.876	
									150.730, −42.693	
									149.659, −43.107	
									151.546, −42.447	
									151.545, −42.447	
									149.659, −43.107	236
1991 Jun 27[c,d]	04:29:23	199.60	−2.60	1.09	134.826	18.423	66.820	0.012	198.986, −3.502	
									199.758, −1.522	
									198.966, −3.488	
									199.734, −1.518	180
1991 Jul 17[c]	04:33:06								247.4875, −59.2052	
									247.2591, −58.1126	
									247.3284, −58.3370	
									247.4138, −58.9874	
									247.4810, −59.2876	
									247.2667, −58.0269	66
1991 Jul 17	13:07:23				320.805	−16.587	89.903	0.252		
1991 Jul 21[b]	19:30:17									
1991 Aug 14[c]	19:14:38								344.4255, 29.0772	
									343.2790, 29.4813	
									343.5043, 29.3878	
									344.1460, 29.1948	
									345.2056, 28.8168	
									342.7718, 29.6208	139
1991 Sep 27[b]	23:27:00	49.70	−42.72	0.94	338.937	−10.074	68.870	0.036	49.326, −43.620	
									49.579, −41.784	
									49.230, −43.595	
									49.482, −41.794	475
1991 Oct 16[a]	11:01:34	297.37	−4.71	0.92					297.996, −5.386	
									298.151, −4.220	
									298.148, −5.205	
									298.251, −4.434	540
1991 Oct 22[b]	04:14:00									
1991 Dec 2[c]	20:28:51	171.97	−22.59	0.94					171.6210, −23.3936	
									173.9107, −22.9482	
									173.7281, −23.0788	
									171.8002, −23.2773	
									171.6010, −23.3436	
									173.9318, −22.9972	707
1991 Dec 9[b]	18:36:11	261.92	−44.19	0.78	348.333	−6.380	82.576	0.003	262.465, −44.866	
									262.520, −43.541	
									262.474, −44.863	
									262.529, −43.545	29

TABLE 2—*Continued*

Date (1)	Time (UT) (2)	WATCH α (3)	WATCH δ (4)	WATCH R (5)	IPN α (6)	IPN δ (7)	IPN R (8)	IPN δR (9)	Error Box Corners (α, δ) (10)	Area (arcmin ^{2}) (11)
1992 Mar 7[b]	00:18:11									
1992 Mar 11[c]	2:20:26	132.25	−36.39	0.33					131.9906, −36.3137	
									132.3481, −36.4731	
									132.1533, −36.3975	
									132.1847, −36.3899	
									132.0761, −36.3403	
									132.2621, −36.4469	15
1992 Mar 25[c]	17:17:37								350.5032, 13.0873	
									350.6150, 13.0463	
									350.5214, 13.0739	
									350.5968, 13.0597	
									350.5757, 13.0725	
									350.5425, 13.0612	4.8
1992 Apr 4[c]	13:11:45	323.07	22.53	0.66					323.2934, 22.4946	
									323.4784, 22.5744	
									323.4180, 22.5292	
									323.3537, 22.5400	
									323.3093, 22.5176	
									323.4625, 22.5515	14.1
1992 Jul 11[c]	16:09:17								281.5245, 72.8744	
									281.5087, 72.8867	
									281.5545, 72.8851	
									281.4786, 72.8760	
									281.4663, 72.8691	
									281.5669, 72.8919	0.92
1992 Jul 14[a]	13:04:33	221.43	−30.75	0.52					220.826, −30.721	
									220.897, −30.506	
									220.848, −30.607	36
1992 Jul 18[b]	14:40:43	21.37	−3.36	0.78	332.718	−4.782	49.196	0.032	22.079, −3.688	
									22.034, −2.949	
									22.019, −3.794	
									21.963, −2.852	175
1992 Jul 18[b]	21:32:44	296.17	−55.95	0.65	332.751	−4.760	58.948	0.004	296.924, −56.446	
									295.262, −55.549	
									296.936, −56.441	
									295.271, −55.542	39
1992 Jul 20[c]	05:53:20	145.67	−11.20	1.09					145.5853, −11.0979	
									145.3282, −10.4052	
									145.0168, −10.8227	
									145.8982, −10.6772	
									146.0366, −10.8810	
									144.8843, −10.6118	1580
1992 Jul 23[b]	01:00:49									
1992 Jul 23[a]	20:03:09	287.08	27.33	0.28					287.128, 27.216	
									287.155, 27.248	
									287.126, 27.210	
									287.157, 27.255	
									287.148, 27.249	
									287.135, 27.215	0.9
1992 Aug 14[b]	06:10:35	259.83	−45.17	1.24	336.053	−2.478	78.143	0.006	260.657, −46.267	
									260.166, −43.953	
									260.672, −46.262	
									260.182, −43.956	95
1992 Sep 2[b]	00:29:02	279.08	−22.81	0.46	338.594	−0.651	61.607	0.015	279.400, −23.163	
									279.212, −22.366	
									279.427, −23.141	
									279.246, −22.376	86
1992 Sep 3	01:35:46	295.87	35.46	0.70	338.740	−0.540	54.168	0.215	295.021, 35.571	
									295.380, 36.036	
									295.215, 35.009	
									296.093, 36.136	855
1992 Sep 3	23:29:01	301.54	22.59	0.30	338.863	−0.453	43.062	0.007	301.344, 22.351	
									301.638, 22.876	
									301.356, 22.343	
									301.652, 22.872	29

TABLE 2—*Continued*

Date (1)	Time (UT) (2)	WATCH α (3)	WATCH δ (4)	WATCH R (5)	IPN α (6)	IPN δ (7)	IPN R (8)	IPN δR (9)	Error Box Corners (α, δ) (10)	Area (arcmin ^{2}) (11)
1992 Sep 25	20:30:42	201.11	42.20	0.76	161.767	−1.864	56.582	0.007	201.776, 41.624	
									200.440, 42.778	
									201.762, 41.615	
									200.426, 42.769	74
1992 Sep 25[b]	21:45:20									
1992 Sep 25	22:46:24	330.80	25.48	0.39	341.779	1.878	25.717	0.086	330.448, 25.255	
									331.214, 25.591	
									330.603, 25.133	
									331.224, 25.404	475
1992 Oct 13	23:00:42	117.71	33.41	0.32	163.948	−3.879	57.350	0.007	117.556, 33.117	
									117.950, 33.660	
									117.572, 33.112	
									117.963, 33.651	32
1992 Oct 22[b]	15:21:00	254.43	−9.64	0.72	164.862	−4.861	88.377	0.002	254.093, −10.279	
									253.993, −9.063	
									254.088, −10.276	
									253.988, −9.067	22
1992 Oct 25	13:55:40				345.153	5.208	27.696	0.013		
1992 Oct 29[b]	12:38:05	35.82	−0.42	1.25	345.514	5.651	50.169	0.045	35.277, −1.546	
									35.594, 0.809	
									35.192, −1.501	
									35.501, 0.789	770
1993 Jan 6[b].....	15:37:40									
1993 Jan 16[b]	02:47:06									
1993 Jun 9[b]	10:07:30									
1993 Jun 12[d,e].....	00:44:20	109.24	−71.20	0.70	143.975	−11.183	63.927	0.053	110.227, −71.826	
									107.144, −71.028	
									110.533, −71.767	
									107.261, −70.922	480
1993 Jul 3	11:26:30	311.06	8.04	0.77	326.006	11.775	15.185	0.044	311.244, 7.292	
									310.830, 8.776	
									311.328, 7.317	
									310.915, 8.797	480
1993 Jul 5[b]	12:39:18									
1993 Jul 6[e]	05:13:31	281.42	−20.18	0.47					281.2524, −20.1137	
									281.2359, −20.0678	
									281.2214, −20.0669	
									281.2669, −20.1146	
									281.2674, −20.1259	
									281.2209, −20.0557	3
1993 Jul 14[b].....	16:13:04									
1993 Sep 10[b]	12:12:30									
1993 Sep 27[b]	04:18:15									
1994 Mar 29[b]	18:15:44									
1994 Apr 19[b].....	19:11:07	358.82	−48.19	1.02	121.768	−46.270	73.314	0.062	357.496, −48.709	
									359.915, −47.483	
									357.601, −48.813	
									0.036, −47.577	906
1994 Jun 19[b]	21:32:32									
1994 Jul 1[b]	21:44:29	145.67	−6.15	1.56	126.479	−39.199	37.139	0.157	147.078, −6.841	
									144.231, −5.530	
									146.909, −7.108	
									144.135, −5.830	3500
1994 Jul 3[b]	04:40:55	133.20	28.11	0.24	126.771	−39.239	67.508	0.005	133.434, 27.988	
									132.944, 28.029	
									133.427, 27.978	
									132.949, 28.018	16
1994 Sep 10	23:57:56				150.200	−51.597	70.732	0.046		

NOTE.—Units of right ascension and declination are degrees.
[a] Localized using *PVO*, SIGMA, and PHEBUS (Hurley et al. 2000a).
[b] *Ulysses*-BATSE error box in Hurley et al. 1999a.
[c] Also observed by and/or localized using *PVO* (Laros et al. 1998).
[d] Also localized by COMPTEL (Kippen et al. 1998).
[e] Also observed by and/or localized using *MO* (Laros et al. 1997).

REFERENCES

Akerlof, C., et al. 1999, Nature, 398, 400
Barat, C., et al. 1988, in AIP Conf. Ser. 170, Nuclear Spectroscopy of Astrophysical Sources, ed. N. Gehrels & G. Share (New York: AIP), 395
Claret, A., et al. 1994, A&A, 287, 824
Costa, E., et al. 1997, Nature, 387, 783
Galama, T., et al. 1998, Nature, 395, 670
Hurley, K., Briggs, M., Kippen, R., Kouveliotou, C., Meegan, C., Fishman, G., Cline, T., & Boer, M. 1999a, ApJS, 120, 399
———. 1999b, ApJS, 122, 497
Hurley, K., et al. 1992, A&AS, 92, 401
———. 2000a, ApJ, 533, 884
Hurley, K., et al. 2000b, ApJ, 534, 258
Kippen, R., et al. 1998, ApJ, 492, 246
Laros, J., et al. 1997, ApJS, 110, 157
———. 1998, ApJS, 118, 391
Meegan, C. A., et al. 1996, ApJS, 106, 65
Paciesas, W. S., et al. 1999, ApJS, 122, 465
Sazonov, S., Sunyaev, R., Terekhov, O., Lund, N., Brandt, S., & Castro-Tirado, A. 1998, A&AS, 129, 1
Terekhov, O., et al. 1991, Adv. Space Res., 11(8), 129
van Paradijs, J., et al. 1997, Nature, 386, 686